Am J Transl Res 2015;7(8):1417-1428
www.ajtr.org /ISSN:1943-8141/AJTR0010361

Original Article

Effects of sequentially released BMP-2 and BMP-7 from PELA microcapsule-based scaffolds on the bone regeneration

Xialin Li[1,2*], Weihong Yi[2*], Anmin Jin[1], Yang Duan[1], Shaoxiong Min[1]

[1]Department of Orthopaedics, Zhujiang Hospital of Southern Medical University, Guangzhou 510282, Guangdong, China; [2]Department of Spine Surgery, Shenzhen Nanshan Hospital of Guangdong Medical College, Shenzhen 510282, Guangdong, China. [*]Equal contributors.

Received May 19, 2015; Accepted July 11, 2015; Epub August 15, 2015; Published August 30, 2015

Abstract: Osteoinductive biomaterials are helpful for the therapy of large bone defects and provide an alternative to autogenous bone and allografts. Recently, multiple growth factors are delivered to mimic the natural process of bone healing in the bone tissue engineering. Herein, we investigated the effects of sequential released bone morphogenetic protein-2 (BMP-2) and bone morphogenetic protein-7 (BMP-7) from polylactide-poly (ethylene glycol)-polylactide (PELA) microcapsule-based scaffolds on the bone regeneration. Through improving the double emulsion/solvent evaporation technique, BMP-7 was encapsulated in PELA microcapsules, to the surface of which BMP-2 was attached. Then, the scaffold (BMP-2/PELA/BMP-7) was fused by these microcapsules with dichloromethane vapor method. *In vitro*, it sequentially delivered bioactive BMP-2 and BMP-7 and partially imitated the profile of BMPs expression during the fracture healing. To determine the bioactivity of released BMP-2 and BMP-7, alkaline phosphatase (AKP) activity was analyzed in MC3T3-E1 cells. When compared with simple BMP-2 plus BMP-7group and pure PELA group, the AKP activity in BMP-2/PELA/BMP-7 group significantly increased. MTT assay indicated the BMP-loaded PELA scaffold had no adverse effects on cell activity. In addition, the effects of BMP-loaded scaffolds were also investigated in a rat femoral defect model by micro-computed tomographic (mCT) and histological examination. At 4 and 8 weeks post-implantation, BMP-2/PELA/BMP-7 significantly promoted osteogenesis as compared to other groups. The scaffold underwent gradual degradation and replacement by new bones at 8 weeks. Our findings suggest that the sequential release of BMP-2 and BMP-7from PELA microcapsule-based scaffolds is promising for the therapy of bone defects.

Keywords: Bone tissue engineering, sequential release, BMPs, PLA-PEG-PLA, PELA, scaffold

Introduction

The treatment of large bone defects due to comminuted fracture, tumor excision, and osteomyelitis still remains a challenge in clinical practice. As a gold standard for the treatment of bone defects, autogenous bone transplantation has some limitations such as donor site pain and limited resource. Transplantation of allogeneic bones is an alternative, but it has high medical cost and risks for virus transmission and adverse immune reactions which significantly limit its wide application [1, 2]. Osteoinductive biomaterials are promising to solve these problems and provide an alternative to autogenous bone and allografts. Some growth factors (such as bone morphogenetic protein-2 [BMP-2] and bone morphogenetic protein-7 [BMP-7]) have been found to promote bone healing. Carriers with growth factors have been applied for the fracture healing and spinal fusion in clinical practice [3-5]. However, some problems warrant resolve after a wide clinical application. For example, local soft tissue edema, spinal radiculitis, ectopic ossification, bone resorption around the implant and risk for cancer are concerns in the use of these carriers [6-10], which might be caused by the unreasonable release of BMPs at a high dose [11]. Thus, it is imperative to develop ideal substitutes to synthetic bone grafts for the clinical application.

Table 1. Microcapsules containing BMPsfor scaffolds fusing

Microcapsules	Wall materials	Encapsulated protein	Covered protein
Group A	280 mg PELA	3 μg rhBMP-7	3 μg rhBMP-2
Group B	280 mg PELA	3 μg rhBMP-7	-
Group C	280 mg PELA	-	3 μg rhBMP-2
Group D	280 mg PELA	-	-

In the natural process of bone healing after a fracture, a variety of growth factors, (such as BMPs, vascular endothelial growth factor [VEGF] and insulin-like growth factor [IGF]) are found to regulate the cellular activities, induce the osteogenic differentiation of mesenchymal stem cells (MCS) and promote the osteogenesis [12-14]. BMP-2 and BMP-7 have been proved to possess a potent osteoinductive activity [11, 15, 16]. Previous studies have indicated that BMP-2 reaches a peak on the first day after a fracture, and BMP-7 increases after 2 weeks in the natural process of bone healing [17]. Recently, some studies show that the combined delivery of BMP-2 and BMP-7 is able to improve the bone regeneration and bone healing after a fracture as compared to the delivery of a single factor [18, 19]. Thus, if scaffolds carrying growth factors can release these growth factors sequentially and slowly in a biomimetic manner, it would optimize the bone defect repair.

The clinic application of BMPs as hydrophilic proteins is often limited by their low bioavailability due to the poor stability and the short biological half-life in the circulatory system [11]. Carriers as delivery system for BMPs are promising to control the release of these factors and provide an initial support for cells and tissue regeneration [20]. In recent years, some groups have successfully attempted to employ various carriers to deliver BMPs for bone regeneration [21-24]. In 2007,Jaklenec et al provided a simple method to construct scaffolds with protein-loaded microspheres alone by using double emulsion/solvent evaporation technique for control release [25]. In the following year, they continued to prepare scaffolds fused by IGF-I and TGF-β1 loaded microcapsules for cartilage tissue engineering [26]. However, no further relevant studies were reported in this field.

In the present study, we modified the method provided by Jaklenec et alto prepare the scaffolds for bone healing [25]. The scaffolds fused directly by BMPs loaded microscapsules were constructed to promote the bone healing. The microcapsules encapsulating BMP-7 were covered by BMP-2. PLA-PEG-PLAtriblock copolymer (PELA) was used as a material for the wall of microcapsule. The scaffolds fused by these microcapsules could deliver BMP-2 and BMP-7 sequentially. We hypothesized that PELA microcapsules carrying BMP-2 and BMP-7 could display an initial burst release of BMP-2 and a subsequent prolonged release of BMP-7, and this porous, bioabsorbable, plastic scaffold could deliver BMP-2 and BMP-7 in dose and time dependent manners to mimic the natural bone regeneration. The kinetics of growth factor release and the degradation of this scaffold were investigated in the present study. The effects of this scaffold on the bone regeneration were investigated *in vitro* in osteoprogenitor cells and *in vivo*in a rat femoral bone defect model.

Materials and methods

Scaffold construction

Preparation of BMP loaded microcapsules: Microcapsules containing recombinant human BMP-7 (rhBMP-7) were constructed using the improved double emulsion/solvent evaporation technique, as previously reported [27]. After the experimental design of response surface, various parameters were optimized to obtain the highest BMP encapsulation efficiency. Briefly, 3 μg of rhBMP-7 (PROSPEC, Israel) was dissolved in 200 μl of distilled water, which was then mixed with 4 ml of dichloromethane containing 280 mg of PELA (MW 20000). After sonication for 20 min, the primary emulsion was added into 40 ml of 0.8% polyvinyl alcohol (PVA) solution and stirred for 40 min. Then, the microparticles were washed, centrifuged thrice, mixed with 2 ml of phosphate buffered saline (PBS, pH 7.4) containing 3 μg of rhBMP-2 (PROSPEC, Israel) and stirred for 10 min. These microparticles were lyophilized overnight and collected. The microcapsules encapsulating BMP-7 and covered by BMP-2 were prepared (BMP-2/PELA/BMP-7). Four groups of microcapsules are listed in **Table 1**.

Scaffold construction: Microcapsules were fused into scaffolds using the dichloromethane vapor method as previously reported [25]. Briefly, 30 mg of microcapsules were placed

into a small dish (35 mm in diameter) which was then sealed in a large one (60 mm in diameter) containing 5 ml of dichloromethane. The scaffolds were incubated for 10 min. After air-drying for 10 min, it was sterilized by ethylene oxide and stored at -20°C until further use. Four groups of scaffolds were prepared with corresponding microcapsules.

In vitro swelling and degradation

The swelling and degradation tests of scaffolds were performed in PBS (pH 7.4) at 37°C. Sixty milligrams of scaffolds were placed into 15-ml tubes containing 10 ml of PBS and incubated at 37°C. The PBS was refreshed once every 3 days. At each time point (1, 2, 5, 8, 11, 14, 18, 22, 26, 32, 39 and 46 days), scaffold was centrifuged and wet weight (Ww) was recorded. Then, the scaffold was lyophilized for 12 h and the dry weigh (Wd) was obtained. The scaffold weight loss was calculated. The swelling ratio was calculated as the wet weight divided by the dry weight (Ww/Wd).

In vitro release of BMPs

The release of BMPs from BMP-2/PELA /BMP-7 was tested *in vitro* in PBS (pH 7.4) at 37°C. Ten milligrams of scaffolds were incubated with 1 mL of PBS in 1.5-ml EP tubesat 37°C. At each time point (1, 2, 4, 8, 12, 16, 22, 28, 35, 42 days), the tubes were centrifuged at 800 rpm for 30 min. The releasate was collected and stored at -20°C until analysis. Then, 1 ml of fresh PBS was added into each EP tube for further testing of the release of BMPs. The concentrations of BMP-2 and BMP-7 in the releasate were measured by using human BMP-7 and BMP-2 Elisa kits (BOSTER, China). The experiments were carried out in triplicate.

Morphology

The microcapsules and scaffold was imaged by using the Hitachi S-3000N scanning electron microscope (SEM). All the samples were mounted on aluminum stubs, coated with gold, and then viewed under a SEM at an accelerating voltage of 20 kV.

Cell activity assay

MC3T3-E1 cells were cultured in a-MEM containing 10% FBS as previously reported [28, 29]. The activity of cells was measured byMTT (3-(4,5-dimethylthiazolyl-2)-2,5-diphenyltetrazolium bromide) assay with MTT assay Kit (BestBio, China). Cells were seeded in 48-well plates at 5×10^4 cell/cm^2 and incubated with 10 mg of scaffolds in every well. The medium was refreshed once every 3 days. Cells were cultured at 37°C in a humidified atmosphere with 5% CO_2. At days 3, 7 and 14, MTT assay was performed according to the manufacturer's instructions. Briefly, 10 μl of MTT was added into each well and incubated for 4 h at 37°C. Then, the supernatant was removed, and 100 μl of dimethylsulfoxide was added to dissolve formazan crystals. After shaking for 10 min, absorbance (OD) was measured at 550 nm. Cells without scaffold treatment served as a positive control and the medium alone served as a blank control. Cell activity = OD (calculated) - OD (blank control). Six wells were prepared for each sample.

Alkaline phosphatase (AKP) activity assay

Scaffolds (10 mg) were incubated with 1 ml of PBSat 37°C. The releasates from scaffolds were sterilized through a filter (0.2 μm, MEMBRANA, German), collected and stored at -20°C until further use, and replaced by 1 ml of fresh PBS every two days. MC3T3-E1 cells (10^4/cm^2) were seeded on 48-well plates and cultured in a-MEM containing 10% FBS. The medium was refreshed once every 2 days and the releasates from scaffolds were added at the same time. After 1 week and 2 weeks, theAKP activity was measured with the AKP assay kit (Jiancheng Bioengineering Institute, China) according to the manufacturer's instructions. Briefly, cells were lysed with 80 μl of 0.05% Triton X-100 and three freeze-thaw cycles, and then 30 μl of lysate was mixed with 50 μl of matrix containing disodium phenyl phosphate and 50 μl of alkaline buffer. After incubation for 15 min at 37°C, 150 μl of reagent containing 4-aminoantipyrine and $K_3Fe(CN)_6$ was added to stop the reaction. AKP activity was measured colorimetrically at 520 nm with a microplate reader (Thermo scientific, USA). Six wells were prepared for each sample.

In vivo experiment

This study was carried out in accordance with the Guide for the Care and Use of Laboratory Animals of the National Institutes of Health (USA). The protocol was approved by the Experimental Animal Welfare and Ethics Management Committee of Southern Medical

University (China). Surgery was performed after chloral hydrate anesthesia, and all efforts were made to minimize suffering.

Twenty-four three-month-old male Wistar rats weighing 350-400 g were purchased from the Experimental Animal Center of Southern Medical University. Twenty-four rats were randomly assigned to four groups (**Table 1**). All rats were allowed to acclimate to the environment for 3 days before surgery. The segmental femoral bone defect model was established as previously described [30]. One experienced surgeon performed all the operations in aseptic conditions. Under general anesthesia by intraperitoneal injection of 10% chloral hydrate at 400 mg/kg, a 1-cm longitudinal incision was made at the lateral right femur. After separating the muscle tissues, the lateral femoral condyle was exposed. A 5 mm × 5 mm unicortical hole was generated at the condyle with a dental bur and filled with 50 mg of biomaterials. No fixationwas used. Then, the underlying musculatures and skin were closed.

After operation, rats were independently housed in cages. Enrofloxacin (10 mg/kg) was administered for 3 days to prevent infection. Weight bearing was allowed in all the rats which were given ad libitum access to food and water after operation. At weeks 4 and weeks 8 postoperatively, 3 rats from each group were euthanized by CO_2 asphyxiation and the femur was harvested for micro-computed tomography (mCT) and histological examination.

Micro CT

All of the femur samples were evaluated by mCT using a ZKKS-MCT-SHARP micro CT (ZhongkeKaisheng Medical Technology, China) with 70 kV p-tube-voltage, 30 W-power and 20-μm resolution. The region of interest (ROI) was centered at the defect site in the distal femur. A 3-dimensional structural reconstruction view of each sample was obtained from the scanned images. The newly formed bone in each group was evaluated by the ratio of bone volume and total defected volume (BV/TV), bone mineral density (BMD) and trabecular number (Tb.N).

Histological examination

The distal femur was fixed in 10% formalin, decalcified with 10% ethylenediaminetetraacetic acid (EDTA), dehydrated in ethanol gradients, embedded in paraffin, and sagittally cut into 5-mm sections followed by hematoxylin and eosin (HE) staining and Masson Trichrome staining. These sections were observed and representative photographs were captured under a light microscope.

Statistical analysis

Statistical analysis was performed with SPSS 19 (SPSS Inc, USA). Data are presented as a mean ± standard deviation (SD). Comparisons among groups were assessed with one-way analysis of variance (ANOVA) followed by Student-Newman-Keuls test. A value of $P<0.05$ was considered statistically significant.

Results and discussion

Morphologies of microcapsules and scaffolds

The microcapsules encapsulating BMP-7 and covered by BMP-2 were successfully prepared by using the modified double emulsion/solvent evaporation technique. The morphology of these microcapsules is shown in **Figure 1A** (SEM). Most of microcapsuleswere smaller than 100 μm in diameter and the median diameter was 40 μm. These microparticles started to fuse together after 2 min in dichloromethane vapor (**Figure 1B**). After 10 min, the microcapsule-based scaffold was over fused and became a sticky mass. A relative smooth surface of scaffold was observed as shown **Figure 1C**. Even after fusion, the underlying structure of spheres' was still visible. As shown in **Figure 1D**, the diameter of inherent poresranged from 50 μm to 200 μm. The porosity of microcapsule-based scaffolds was reported to be mainly associated with the size of microcapsules and the time of fusion [25]. Studies have established that the architecture of synthetic scaffold need interconnected porosity with the size of 100 μm or greater for vascularization and cell penetration [31]. Small pores favor hypoxic conditions and may promote ion and liquid diffusion [32, 33]. Thus, the porosity of our scaffold would probably be helpful for both penetration of tissue fluid and microvascular ingrowth.

The dichloromethane vapor was utilized to soften the polymer microcapsule and lower the polymer glass transition temperature [25]. In the large the scaffold was plastic and extendable. These properties would help the repair of bone defects with different shapes and sizes. When the dichloromethane was removed, the

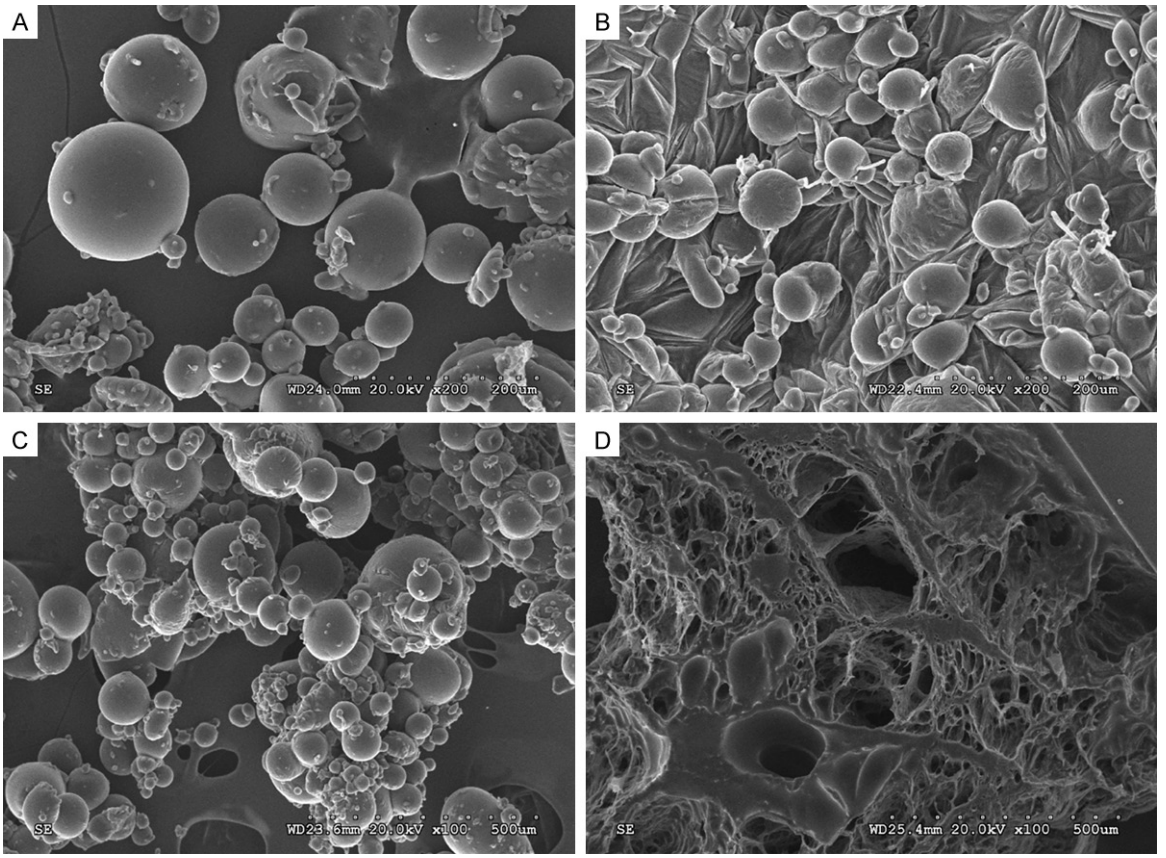

Figure 1. SEM of PELA microcapsules and fused scaffolds: A. BMPs loaded microcapsules; B. Scaffold fused by microcapsules for 2 min; C. Scaffold fused by microcapsules for 10 min; D. Cross-section of scaffolds.

scaffold began to harden again. The whole process needed neither conventional chemical reagent (such as cross-linking agent or pore-foaming agent) nor physical cross-linking reaction (such as infrared light irradiation, UV light exposure and 60 Co radiation). Thus, this preparation can savecost for scaffold preparation and minimize the loss of biological activities of growth factors. Furthermore, this scaffold can be constructed with microcapsules containing various growth factors with modular design, which seems to be extremely valuable for tissue engineering and drug delivery. As a volatile liquid with hypotoxicity, dichloromethane vapor is the only chemical reagent used in scaffold construction. After fusion, the scaffolds were air-dried for 10 min to evaporate the residual dichloromethane completely.

Swelling and degradation of scaffolds

The swelling ratio and change in dry weight of scaffolds in PBS at 37°C were recorded for 46 days. **Figure 2B** showed the swelling ratio of PELA scaffold within 42 days. In the first two weeks, the swelling ratio increased significantly and reached a peak on day 14. Thereafter, it began to decrease gradually and reached a low level at 4 weeks which was maintained. The weight loss of scaffolds is showed in **Figure 2A**. There was no significant weight loss before day 12, which corresponded to the increased swelling ratio. Thereafter, the weight began to decease and 50% weight loss was observed on day 22. After a plateau, the weight loss continued.

An ideal biomaterial for bone regeneration should have a proper degradation rate matching the bone growth. Many factors such as scaffold porosity, temperature and degradation medium can affect the degradation rate [32, 34]. As the triblock polymers composed of biodegradable PLA and inlaid hydrophilic PEG block, PELA has been successfully used as materials in carries of both hydrophilic and

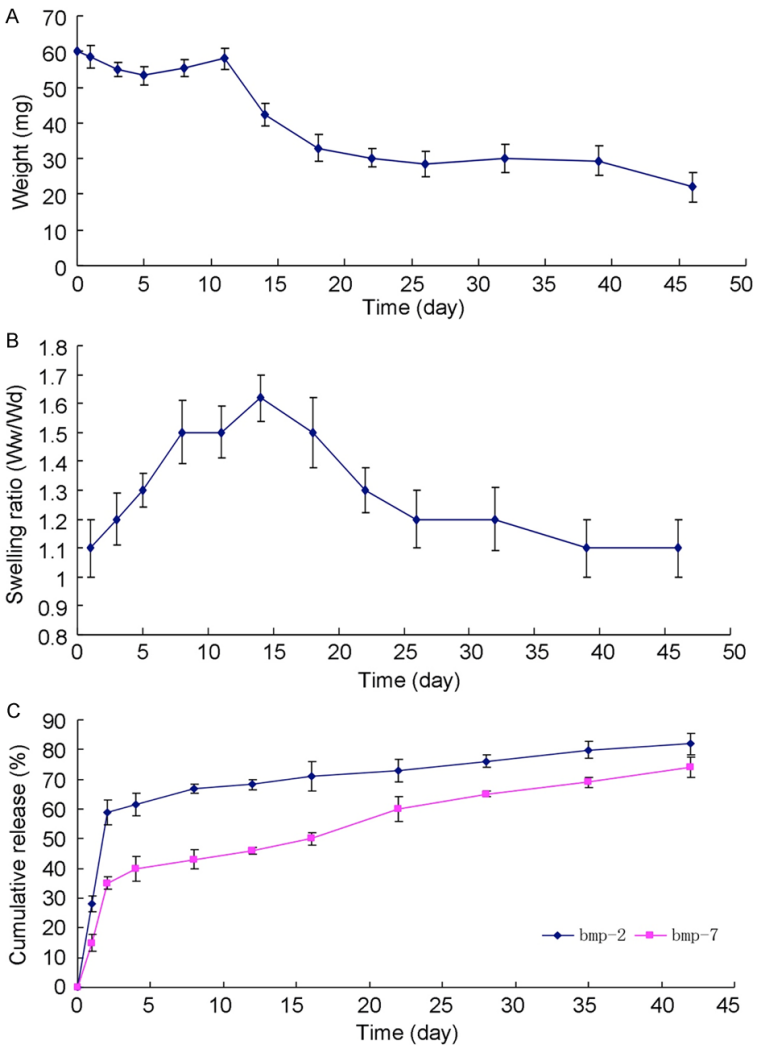

Figure 2. Weigh loss (A), swelling ratio (B) and cumulative release profile (C) of BMP-2/PELA/BMP-7 scaffolds in PBS at 37 °C.

hydrophobic drugs and available findings demonstrate it has favorable properties for the controlled release of drugs [35-37]. In this study, PELA was employed as the materials of microcapsules' wall and PBS (pH 7.4) as the degradation medium. Based on the *in vitro* swelling profile and weigh loss profile, fast degradation was achieved at week 2 after initial swelling, which was similar to previously reported [38, 39].

In vitro BMPs release

To determine whether the release of BMPs from scaffolds mimics the release profile in natural process of fracture healing, the *in vitro* release kinetics of BMP-2 and BMP-7 was measured in BMP-2/PELA/BMP-7 scaffold (**Figure 2C**). As being attached to the surface of microcapsules, BMP-2 had a burst release (60%) on day 2, followed by a persistent release until the end of experiment. The total cumulative release of BMP-2 was 81% after 42 days. The release profile of BMP-7 was different. Although there was still an initial burst release, its release was relatively low on day 2 (32%). Then, the release rate was kept at about 1% per day. Of interest, an accelerated release of BMP-7 was found at week 2, which coincided with the time point at which scaffold swellingbegan to decrease and weight loss was present. After 3 weeks, theBMP-7 release reached the plateau again. At day 42, the cumulative release of BMP-7 reached 74%.

In the scaffold, BMP-2 was designed to adhere to the surface of PELA microcapsuleswhich was responsible for the early burst release, and BMP-7 was encapsulated by the microcapsules, which was responsible for the sustained release. When these microparticles were fused to form porous scaffold, the release was prolonged because some microcapsules was embedded in the scaffold. According to the *in vitro* release profile of BMP-2/PELA/BMP-7 scaffold, BMP-2 had the classic initial burst release followed by a sustained release for more than 42 days. This release profile has been reported to improve the bone regeneration as compared to a sustained release without a burst [40]. Because BMP-7 is encapsulated in PELA microcapsules, the burst release of BMP-7 was partially suppressed and reduced to halfof that of BMP-2. After 12 days, anaccelerated release of BMP-7 maintained for about one week, which would be as a result of degradation of PELA wall and release of residual protein inside the microcapsules. Thus, the release kinetics of BMP-2 and BMP-7 in BMP-2/PELA/BMP-7 scaffolds was

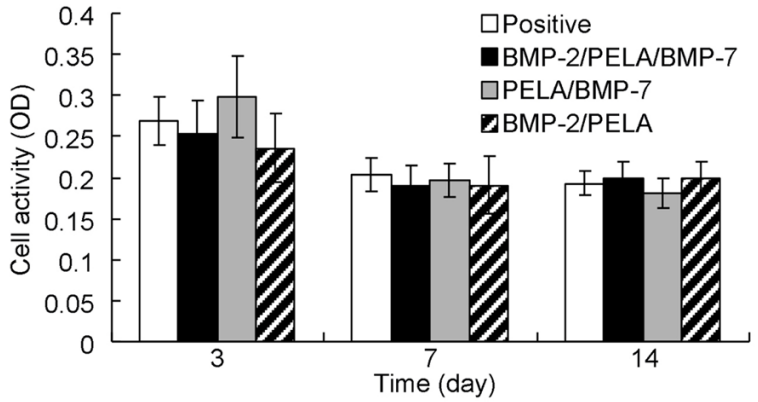

Figure 3. *In vitro* viability of MC3T3-E1 cells incubated with PELA scaffolds (MTT assay). Cells without scaffolds served as a positive control.

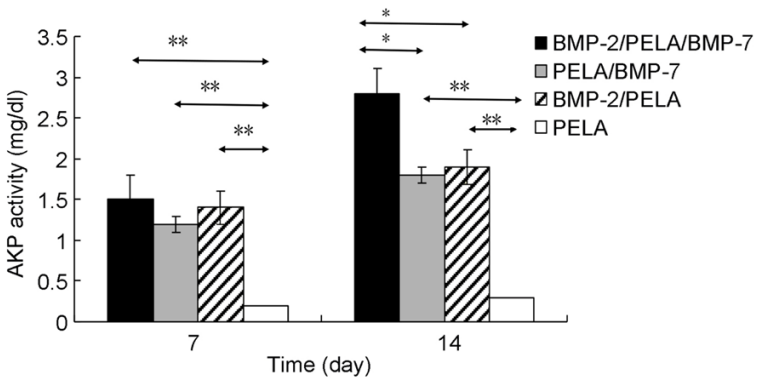

Figure 4. *In vitro* AKP activity of releasates of BMP-2/PELA/BMP-7scaffolds. Releasates from each scaffold was added into medium every 2 days and AKP activity was measured at 7 and 14 days. *P<0.05 and **P<0.01.

similar to the release profile of BMP in natural process of fracture healing and partially mimicked the clinical fracture condition. However, in the actual clinical condition, bone repair and regeneration are complex and have involvement of various healing factors which may interact with each other. Thus, complete imitation is nearly impossible at present.

The advantage ofmicrocapsule-based scaffold is that the release of BMPs from the capsules is controlled by the propertiesof capsule wall. BMP-2 wasattached to the surface of microcapsules, and its release profile depends largely onits affinity to the wall. The thickness of microcapsules and the degradation velocity of materials determine the release kinetics of BMP-7. In addition, the diameter of particles and the fusion time may affect the release curve of proteins [25]. Thus, the release could be fine-tuned by changing the capsule's properties. PELA was choosedas a wall material because it began to degrade rapidly after 12 days *in vitro* which matches the time profile of BMP-7 expression during the bone healing. The encapsulation of BMP-7 made its initial burst releasebe suppressed successfully. Therefore, the release profile of active factors in this model could be optimized constantly to meet the requirement for bone tissue engineering.

In vitro cell viability

To investigate the cytotoxicity of PELA scaffolds, MTT assay was used to evaluate the viability of MC3T3-E1 cells at 3, 7 and 14 days. As shown in **Figure 3**, cell viability was comparable between PELA scaffolds and positive control at all time points. At 3 days, the cell viability increased in group B as compared to pure cells group although there was no significant difference. These results indicate the BMPs loaded PELA scaffolds have no adverse impact on the cell viability within first 2 weeks.

In vitro bioactivity of released BMPs

To investigate the bioactivity of released BMPs from BMPs/PELA scaffolds, MC3T3-E1 cells were employed, the releasates were harvested from 4 groups of scaffolds and the AKP activity was measured at 7 and 14 days. As shown in **Figure 4**, the releasates of Groups A, B and C had markedly enhanced AKP activity at 7 days as compared to Group D ($p<0.01$). All the BMPs loaded scaffolds had markedly enhanced AKP activity as compared to pure PELA group. These results indicate that BMPs' activity is well preserved. At 14 days, the AKP activity in Group A was significantly higher than in Group B and Group C ($P<0.01$), which indicates that BMP-2 and BMP-7 havesynergistic effect to promote

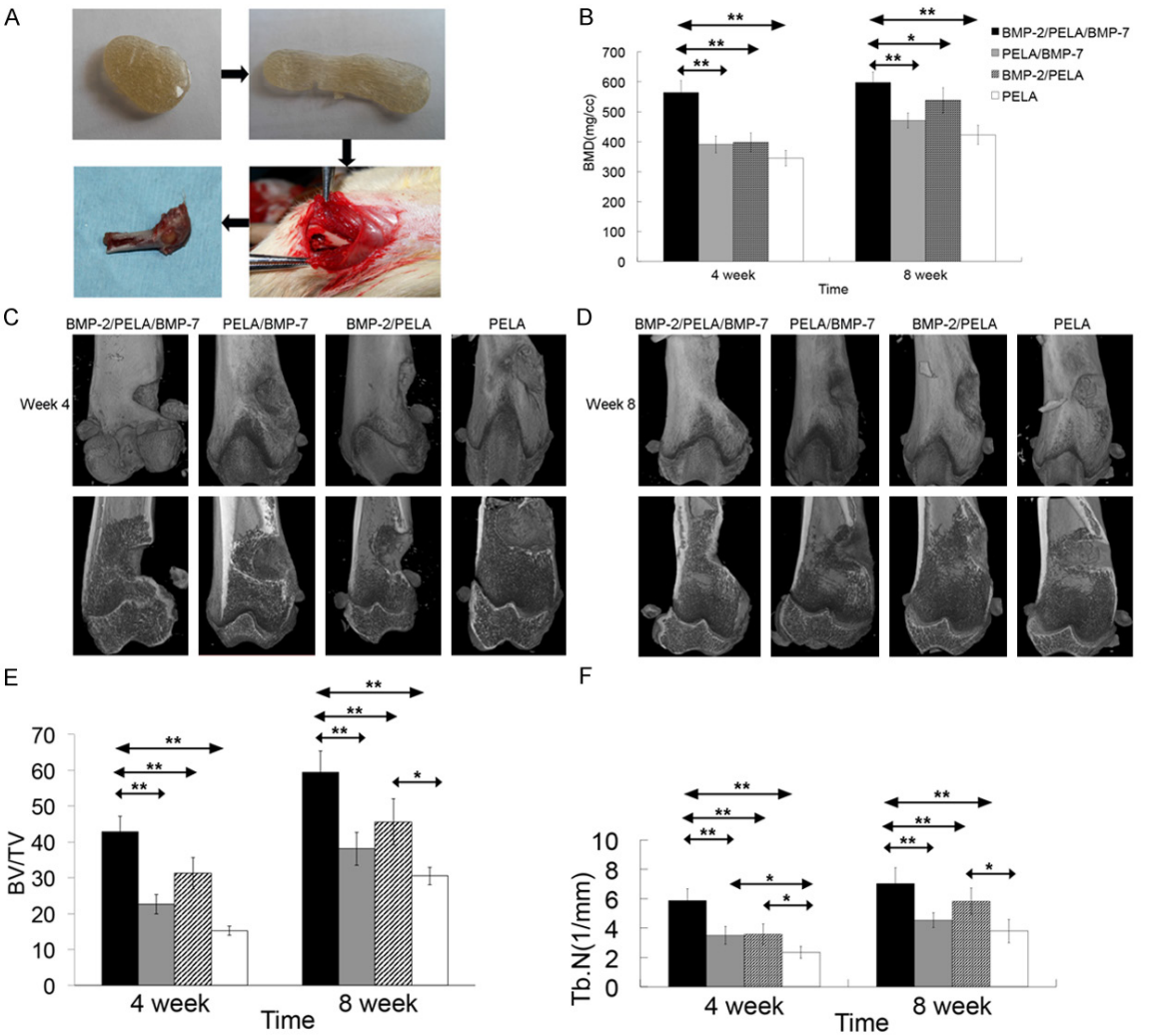

Figure 5. *In vivo* evaluation of bone formation by mCT. A rat femoral defect model was established. Rats were treated with BMP-2/PELA/BMP-7, PELA/BMP-7, BMP-2/PELA and PELA alone. The extendable PELA scaffold was implanted into the defects (A), and the femur was collected for mCT at week 4 (C) and week 8 (D). Bone mineral density (B), ratio of bone volume and total defected volume (E) and trabecular number (F) were used to evaluate the new bone formation in each group. *P<0.05) and **P<0.01.

theosteogenic differentiation of MC3T3-E1 cells.

Therapeutic effects of scaffold in rat femoral defect model

To investigate the effects of BMP/PELA scaffold on the bone regeneration, a bone defect model was established in Wistar rats and 50 mg of scaffolds were implanted at the defect (**Figure 5A**). At week 4, mCT showed the new bone ingrowth in the femoral defectwas more obvious in Group A than in other groups (**Figure 5C**). New bone formation in the Groups B and C were more evident than in Group D at week 4, which implies BMP-2 and BMP-7 released from scaffolds have intact bioactivity and are able to promote new bone formation as compared to control group. At week 8,the new bone formation was more obvious in BMPs combined groups than that at week 4. The femoral hole in Group A was covered completely by new bone tissues, and full-thickness cortical bone was found (**Figure 5D**). Thenew bone formation was more obvious in Groups B and C as compared to that at 4 weeks. The cross section of the bone defect showed the scaffolds in Group C seemed to have stronger ability to promote bone repair than those in Group B, although significant difference was not found. As for

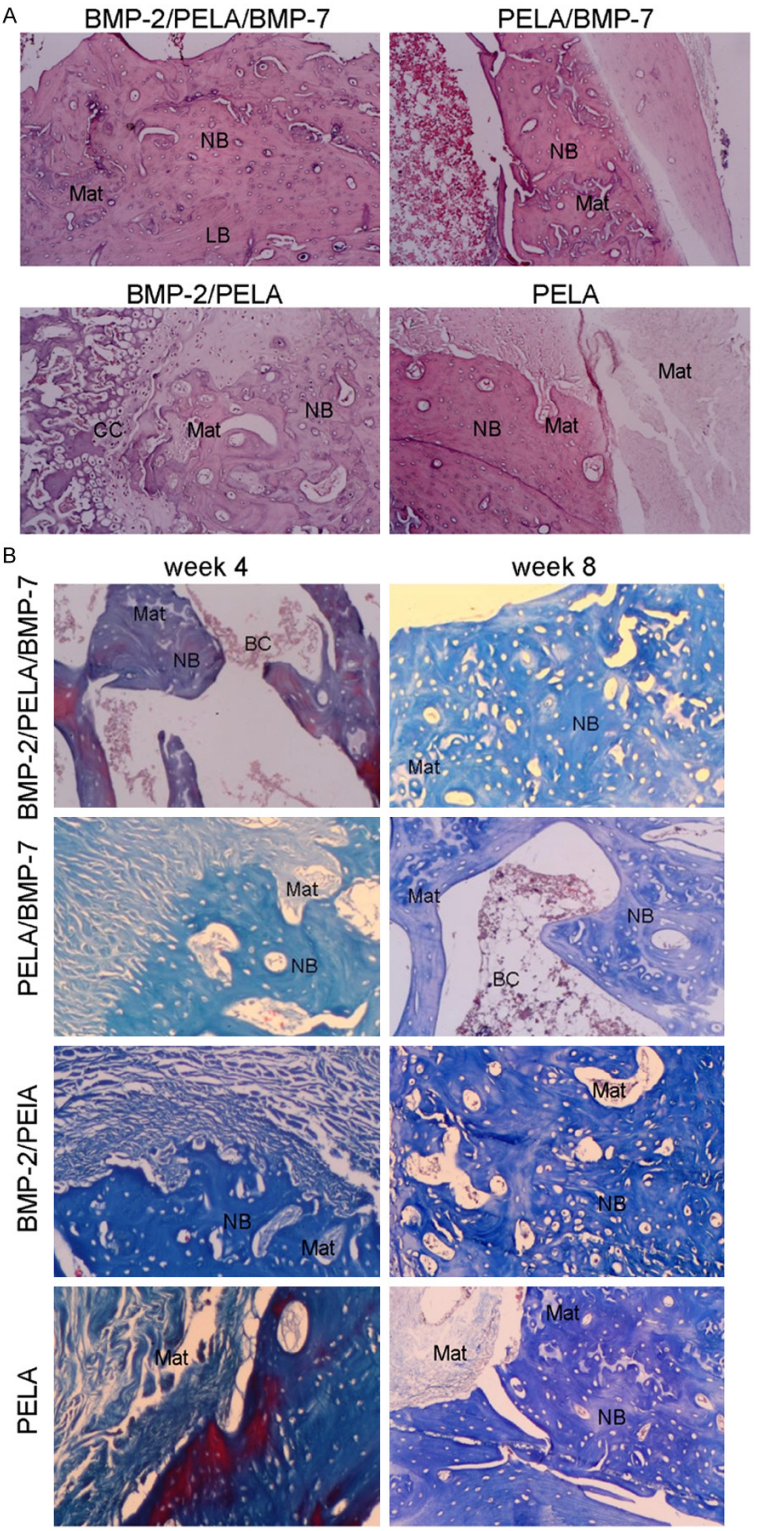

Figure 6. Histological evaluation of new bone formation. BMP-2/PELA/BMP-7, PELA/BMP-7, BMP-2/PELA and PELA scaffolds were independently implanted into defects. The femur was harvested at 4 and 8 weeks, and processed for H&E staining (A) and Masson Trichrome staining (B). (Mat: material, NB: new bone, BC: blood cell, LB: lamellar bone, CC: cartilage cells). Original magnification: 400×.

Group D, there was no obvious new bone formation at week 4. Until 8 weeks, partial new bone ingrowth was found at the defect site.

The regenerated BMD, BV/TV and Tb.N were calculated for the evaluation of new bone formation. As shown in **Figure 5B**, an increase in BMD was observed in all groups, among which Group A had a higher BMD than Groups B, C and D at each time point ($P<0.01$). Groups B and C showed a higher BMC than Group D at week 4 ($P<0.01$) and week 8 ($P<0.05$). Of interest, Group C had a higher BMD than Group B at 8 weeks ($P<0.05$). Similar trend was found in **Figure 5E** and **5F**. Group A hadhigher BV/TV and Tb.N than other groups at each time point ($P<0.01$), and Group C demonstrated higher BV/TV and Tb.N than Group D at 8 weeks ($P<0.05$). These findings suggest that BMP-2/PELA/BMP-7 scaffolds may achieve larger new bone volume and higher bone quality as compared to scaffolds with a single growth factor, which consist with previous findings [41, 42]. In addition, BMP-2/PELA scaffolds seemed to show a better ability to enhance bone healing than PELA/BMP-7 scaffolds in the long run.

Actually, some groups have attempted to employ carriers with both BMP-2 and BMP-7 to regulate osteogenic differentiation [18, 42-44]. Most of studies conclude that the sequential delivery of growth factors is a better approach for bone tissue engineering. In the present study, the microcapsule-based scaffolds were employed to prepare the

BMP-2/BMP-7 delivery system with a simple method. Results indicated the sequential release of BMP-2 and BMP-7 from these scaffolds could effectively promote bone healing *in vivo*.

Histological examination

To evaluate the newly formed bone tissue, histological examination of the femur was performed in rats with femoral bone defect after implantation of these scaffolds. In Group A, new bone was observed around the residual materials containing a plenty of blood cells at 4 weeks. The copolymers seemed to degrade along with new bone formation. At week 8,more and thicker new bone was observed and tended to become lamellar bone (**Figure 6A**). Some osteons with vessels were seen in the bone matrix. Only a little degradation products of materials were found to be surrounded by new bone tissues. Then, its biodegradability and biocompatibility were further investigated which was in agreement with previous studies [35, 36, 45, 46]. In both Groups B and C, limited new woven bone with materials was observed in the bone matrix at week 4 (**Figure 6B**). The replacement of degraded materials by new bone tissues were seen clearly. At week 8, more new bone was observed, but no matured lamellar bone was found in both groups. In Group D, no new bone formation was found and only some fibrous membranes existed between old bone tissues and materials at week 4 (**Figure 6B**). Until week 8, new bone tissues began to appear and replace the biomaterials (**Figure 6A** and **6B**), confirming the findings from 3D mCT.

Conclusion

In this study, we successfully construct biodegradable PELA scaffolds fused by BMPs-loaded microcapsules which are then used to repair bone defect in rat femoral bone defect model. With the modified double emulsion/solvent evaporation technique BMP-7 is encapsulated in PELA microcapsules and BMP-2 is attached to the surface of these microparticles. The porous scaffolds fused directly by these microcapsules can deliver BMP-2 and BMP-7 sequentially and partiallyimitate the profile of BMPs expression during fracture healing. Bioactive BMPs show a controlled release within at least 42 days. This delivery system may exert synergistic effect to promoteosteogenic differentiation of MC3T3-E1 cells'*in vitro* and repair the bone defect *in vivo*. These results indicate that the BMP-2/PELA/BMP-7 scaffolds have a potential for the clinical repair of large bone defects.

Acknowledgements

This work was supported by the central laboratory of the Anatomy Research Institution in Southern Medical University, and funded by Guangdong Natural Science Foundation (No. 2014A030313348) and scientific research projects of Shenzhen Health family planning system (No. 201505026). The authors thank Weiyi Huang and Wenbing Wan for their assistance with animal surgeries and cell experiments.

Disclosure of conflict of interest

None.

Address correspondence to: Shaoxiong Min, Department of Orthopaedics, Zhujiang Hospital of Southern Medical University, No.253 Gongye Road, Guangzhou 510282, Guangdong, China. Tel: 86 13823210257; Fax: 86 13928885822; E-mail: minshaoxiong@126.com

References

[1] Liu X, Rahaman MN and Fu Q. Bone regeneration in strong porous bioactive glass (13-93) scaffolds with an oriented microstructure implanted in rat calvarial defects. Acta Biomater 2013; 9: 4889-4898.

[2] Giorgini A, Donati D, Cevolani L, Frisoni T, Zambianchi F and Catani F. Fresh osteochondral allograft is a suitable alternative for wide cartilage defect in the knee. Injury 2013; 44 Suppl 1: S16-20.

[3] White AP, Vaccaro AR, Hall JA, Whang PG, Friel BC and McKee MD. Clinical applications of BMP-7/OP-1 in fractures, nonunions and spinal fusion. Int Orthop 2007; 31: 735-741.

[4] McKay WF, Peckham SM and Badura JM. A comprehensive clinical review of recombinant human bone morphogenetic protein-2 (INFUSE Bone Graft). Int Orthop 2007; 31: 729-734.

[5] Nyberg E, Holmes C, Witham T and Grayson WL. Growth factor-eluting technologies for bone tissue engineering. Drug Deliv Transl Res 2015; [Epub ahead of print].

[6] Carlisle E and Fischgrund JS. Bone morphogenetic proteins for spinal fusion. Spine J 2005; 5: 240S-249S.

[7] Lebl DR. Bone morphogenetic protein in complex cervical spine surgery: A safe biologic adjunct? World J Orthop 2013; 4: 53-57.
[8] Cahill KS, Chi JH, Day A and Claus EB. Prevalence, complications, and hospital charges associated with use of bone-morphogenetic proteins in spinal fusion procedures. JAMA 2009; 302: 58-66.
[9] Lad SP, Bagley JH, Karikari IO, Babu R, Ugiliweneza B, Kong M, Isaacs RE, Bagley CA, Gottfried ON, Patil CG and Boakye M. Cancer after spinal fusion: the role of bone morphogenetic protein. Neurosurgery 2013; 73: 440-449.
[10] Michielsen J, Sys J, Rigaux A and Bertrand C. The effect of recombinant human bone morphogenetic protein-2 in single-level posterior lumbar interbody arthrodesis. J Bone Joint Surg Am 2013; 95: 873-880.
[11] Calori GM, Donati D, Di Bella C and Tagliabue L. Bone morphogenetic proteins and tissue engineering: future directions. Injury 2009; 40 Suppl 3: S67-76.
[12] Kim IS, Cho TH, Lee ZH and Hwang SJ. Bone regeneration by transplantation of human mesenchymal stromal cells in a rabbit mandibular distraction osteogenesis model. Tissue Eng Part A 2013; 19: 66-78.
[13] Fowlkes JL, Nyman JS, Bunn RC, Jo C, Wahl EC, Liu L, Cockrell GE, Morris LM, Lumpkin CK Jr and Thrailkill KM. Osteo-promoting effects of insulin-like growth factor I (IGF-I) in a mouse model of type 1 diabetes. Bone 2013; 57: 36-40.
[14] Clarkin CE and Gerstenfeld LC. VEGF and bone cell signalling: an essential vessel for communication? Cell Biochem Funct 2013; 31: 1-11.
[15] Bessa PC, Casal M and Reis RL. Bone morphogenetic proteins in tissue engineering: the road from the laboratory to the clinic, part I (basic concepts). J Tissue Eng Regen Med 2008; 2: 1-13.
[16] Kim DY, Kim JR, Jang KY and Lee KB. A new concept for implant fixation: bone-to-bone biologic fixation. Eur Cell Mater 2015; 29: 281-289.
[17] Cho TJ, Gerstenfeld LC and Einhorn TA. Differential temporal expression of members of the transforming growth factor beta superfamily during murine fracture healing. J Bone Miner Res 2002; 17: 513-520.
[18] Yilgor P, Tuzlakoglu K, Reis RL, Hasirci N and Hasirci V. Incorporation of a sequential BMP-2/BMP-7 delivery system into chitosan-based scaffolds for bone tissue engineering. Biomaterials 2009; 30: 3551-3559.
[19] Ehnert S, Zhao J, Pscherer S, Freude T, Dooley S, Kolk A, Stockle U, Nussler AK and Hube R. Transforming growth factor beta1 inhibits bone morphogenic protein (BMP)-2 and BMP-7 signaling via upregulation of Ski-related novel protein N (SnoN): possible mechanism for the failure of BMP therapy? BMC Med 2012; 10: 101.
[20] Lin X, de Groot K, Wang D, Hu Q, Wismeijer D and Liu Y. A review paper on biomimetic calcium phosphate coatings. Open Biomed Eng J 2015; 9: 56-64.
[21] Ben-David D, Srouji S, Shapira-Schweitzer K, Kossover O, Ivanir E, Kuhn G, Muller R, Seliktar D and Livne E. Low dose BMP-2 treatment for bone repair using a PEGylated fibrinogen hydrogel matrix. Biomaterials 2013; 34: 2902-2910.
[22] Cao L, Wang J, Hou J, Xing W and Liu C. Vascularization and bone regeneration in a critical sized defect using 2-N,6-O-sulfated chitosan nanoparticles incorporating BMP-2. Biomaterials 2014; 35: 684-698.
[23] Cha JK, Lee JS, Kim MS, Choi SH, Cho KS and Jung UW. Sinus augmentation using BMP-2 in a bovine hydroxyapatite/collagen carrier in dogs. J Clin Periodontol 2014; 41: 86-93.
[24] de Guzman RC, Saul JM, Ellenburg MD, Merrill MR, Coan HB, Smith TL and Van Dyke ME. Bone regeneration with BMP-2 delivered from keratose scaffolds. Biomaterials 2013; 34: 1644-1656.
[25] Jaklenec A, Wan E, Murray ME and Mathiowitz E. Novel scaffolds fabricated from protein-loaded microspheres for tissue engineering. Biomaterials 2008; 29: 185-192.
[26] Jaklenec A, Hinckfuss A, Bilgen B, Ciombor DM, Aaron R and Mathiowitz E. Sequential release of bioactive IGF-I and TGF-beta 1 from PLGA microsphere-based scaffolds. Biomaterials 2008; 29: 1518-1525.
[27] Li X, Min S, Zhao X, Lu Z and Jin A. Optimization of entrapping conditions to improve the release of BMP-2 from PELA carriers by response surface methodology. Biomed Mater 2014; 10: 015002.
[28] Lee H, Ahn S, Bonassar LJ and Kim G. Cell (MC3T3-E1)-printed poly (-caprolactone)/alginate hybrid scaffolds for tissue regeneration. Macromol Rapid Commun 2013; 34: 142-149.
[29] Mai Z, Peng Z, Wu S, Zhang J, Chen L, Liang H, Bai D, Yan G and Ai H. Single bout short duration fluid shear stress induces osteogenic differentiation of MC3T3-E1 cells via integrin beta1 and BMP2 signaling cross-talk. PLoS One 2013; 8: e61600.
[30] Li B, Yoshii T, Hafeman AE, Nyman JS, Wenke JC and Guelcher SA. The effects of rhBMP-2 released from biodegradable polyurethane/microsphere composite scaffolds on new bone formation in rat femora. Biomaterials 2009; 30: 6768-6779.

[31] Lan Levengood SK, Polak SJ, Poellmann MJ, Hoelzle DJ, Maki AJ, Clark SG, Wheeler MB and Wagoner Johnson AJ. The effect of BMP-2 on micro- and macroscale osteointegration of biphasic calcium phosphate scaffolds with multiscale porosity. Acta Biomater 2010; 6: 3283-3291.

[32] Karageorgiou V and Kaplan D. Porosity of 3D biomaterial scaffolds and osteogenesis. Biomaterials 2005; 26: 5474-5491.

[33] Mathieu LM, Mueller TL, Bourban PE, Pioletti DP, Muller R and Manson JA. Architecture and properties of anisotropic polymer composite scaffolds for bone tissue engineering. Biomaterials 2006; 27: 905-916.

[34] Yang F, Wang J, Hou J, Guo H and Liu C. Bone regeneration using cell-mediated responsive degradable PEG-based scaffolds incorporating with rhBMP-2. Biomaterials 2013; 34: 1514-1528.

[35] Danafar H, Rostamizadeh K, Davaran S and Hamidi M. PLA-PEG-PLA copolymer-based polymersomes as nanocarriers for delivery of hydrophilic and hydrophobic drugs: preparation and evaluation with atorvastatin and lisinopril. Drug Dev Ind Pharm 2014; 40: 1411-20.

[36] Liu Z, Gao X, Kang T, Jiang M, Miao D, Gu G, Hu Q, Song Q, Yao L, Tu Y, Chen H, Jiang X and Chen J. B6 peptide-modified PEG-PLA nanoparticles for enhanced brain delivery of neuroprotective peptide. Bioconjug Chem 2013; 24: 997-1007.

[37] Oak M and Singh J. Chitosan-zinc-insulin complex incorporated thermosensitive polymer for controlled delivery of basal insulin in vivo. J Control Release 2012; 163: 145-153.

[38] Liu S, Hu C, Li F, Li XJ, Cui W and Fan C. Prevention of peritendinous adhesions with electrospun ibuprofen-loaded poly(L-lactic acid)-polyethylene glycol fibrous membranes. Tissue Eng Part A 2013; 19: 529-537.

[39] Maquet V, Martin D, Scholtes F, Franzen R, Schoenen J, Moonen G and Jer me R. Poly(D,L-lactide) foams modified by poly(ethylene oxide)-block-poly(D,L-lactide) copolymers and a-FGF: in vitro and in vivo evaluation for spinal cord regeneration. Biomaterials 2001; 22: 1137-1146.

[40] Brown KV, Li B, Guda T, Perrien DS, Guelcher SA and Wenke JC. Improving bone formation in a rat femur segmental defect by controlling bone morphogenetic protein-2 release. Tissue Eng Part A 2011; 17: 1735-1746.

[41] Kaito T, Johnson J, Ellerman J, Tian H, Aydogan M, Chatsrinopkun M, Ngo S, Choi C and Wang JC. Synergistic effect of bone morphogenetic proteins 2 and 7 by ex vivo gene therapy in a rat spinal fusion model. J Bone Joint Surg Am 2013; 95: 1612-1619.

[42] Huri PY, Huri G, Yasar U, Ucar Y, Dikmen N, Hasirci N and Hasirci V. A biomimetic growth factor delivery strategy for enhanced regeneration of iliac crest defects. Biomed Mater 2013; 8: 045009.

[43] Hakki SS, Bozkurt B, Hakki EE, Kayis SA, Turac G, Yilmaz I and Karaoz E. Bone morphogenetic protein-2, -6, and -7 differently regulate osteogenic differentiation of human periodontal ligament stem cells. J Biomed Mater Res B Appl Biomater 2014; 102: 119-30.

[44] Yilgor P, Yilmaz G, Onal MB, Solmaz I, Gundogdu S, Keskil S, Sousa RA, Reis RL, Hasirci N and Hasirci V. An in vivo study on the effect of scaffold geometry and growth factor release on the healing of bone defects. J Tissue Eng Regen Med 2013; 7: 687-696.

[45] Kutikov AB and Song J. An amphiphilic degradable polymer/hydroxyapatite composite with enhanced handling characteristics promotes osteogenic gene expression in bone marrow stromal cells. Acta Biomater 2013; 9: 8354-8364.

[46] Garofalo C, Capuano G, Sottile R, Tallerico R, Adami R, Reverchon E, Carbone E, Izzo L and Pappalardo D. Different Insight into Amphiphilic PEG-PLA Copolymers: Influence of Macromolecular Architecture on the Micelle Formation and Cellular Uptake. Biomacromolecules 2014; 15: 403-15.